

Network mechanisms of dynamic feature selection for flexible visual categorizations

Y. Duan⁽¹⁾, J. Zhan⁽¹⁾, J. Gross⁽²⁾, R.A.A. Ince⁽¹⁾ & P.G. Schyns^(1*)

(1) School of Psychology and Neuroscience, University of Glasgow, United Kingdom

(2) Institute for Biomagnetism and Biosignalanalysis, University of Münster, Germany

(*)Corresponding author

Philippe G. Schyns
School of Psychology and Neuroscience
58, Hillhead Street
University of Glasgow
Glasgow G128AB
United Kingdom
+44 141 330 4937

Abstract

Visual categorization is the pervasive cognitive function with which humans make sense of their external world. Current theories and models assume that the visual hierarchy reduces its high-dimensional input, by flexibly selecting the stimulus features that support categorization behavior. To investigate such feature selection, we quantified top-down task effects on the dynamic representation of stimulus features. We recorded the MEG as participants categorized the same scene images in different ways (in blocks of *face expression*, *face gender*, *pedestrian gender*, and *vehicle type* trials, within-participant). We show where, when and how brain networks select categorization features. Specifically, occipital MEG sources represent all stimulus features ~50-170ms post-stimulus, but with opponent response, to select or reduce the same stimulus features depending on their task-relevance. Following this 170 ms junction, occipito-ventral and dorsal sources represent only task-relevant features for behavior. Our results therefore show how systems-level network mechanisms dynamically reduce input dimensionality for behavior, by selecting task-relevant stimulus features.

The biological machinery that performs human visual categorization has an astonishing range of competences, supported by the most sophisticated of sensory systems. Theories and models suggest that categorization behavior results from brain networks that process the stimulus features that are relevant to each categorization task—i.e. the so-called “diagnostic” features^{1–9}. For example, whereas categorizing the example scene in Figure 1 as a “happy face” requires processing the mouth of the central face, categorizing the same picture as a “SUV” requires processing the shape of the right-flanked vehicle, or the left “female pedestrian” with the bodily features that disclose its gender, and so forth. The key point is that a single input image, and even a single object within an image, typically affords multiple different categorizations (e.g. “happy,” or “female” face), that each result from brain networks flexibly processing different task-relevant features.

To understand the mechanisms of categorization, we need to understand *where*, *when* and particularly *how* these networks flexibly process the features relevant to each behavior. There has been considerable progress in mapping the different regions of the occipito-ventral/dorsal pathways that represent different categories of stimulus pictures (i.e. faces, objects and scenes), from their early split projection in left and right occipital cortex to their categorical-semantic representations in the right fusiform gyrus, and also how feedback could reverse this flow to predict the input^{10–12}. However, the brain mechanisms that dynamically select the specific stimulus features that support each categorization task remain unclear. Converging evidence from eye movement research^{13,14}, endogenous attention^{15,16}, reverse correlation^{17–19} and neural network modelling suggest that categorization mechanisms in a capacity-limited system must adaptively reduce the high-dimensional input stimulus into the low-dimensional features that represent the information required to accomplish each specific categorization task—cf. in Figure 1A, process the mouth feature to respond “happy face,” the vehicle shape to respond “SUV” and bodily features to respond “female pedestrian.” Here, we studied where, when and how brain networks differently reduce stimulus information to perform categorization behavior.

To study these mechanisms, we explicitly characterized the stimulus features that each participant processes to flexibly categorize the same stimuli in four different ways (i.e. *face expression*, *face gender*, *pedestrian gender* and *vehicle type*, see Figure 1). Then, we analyzed where, when and how the participant’s brain networks represent these features, when they are task-relevant (e.g. vehicle feature in *vehicle type* categorization) and when they are not (e.g. the vehicle feature in the *face gender* task). Crucially, we use the same sampled stimuli in each task—i.e. the bottom-up input is the same, only the task changes. To preview our results, we reveal that the task changes feature representations throughout,

from the earliest representations in occipital cortex to later representation in higher-order regions in ventral, dorsal and frontal areas. Prior to 170 ms, occipital cortex sources represent the same feature with an opposite sign of amplitude response, to *select* the feature when it is task-relevant, and to *reduce* it when it is task-irrelevant. Following 170 ms, task-relevant features are *selected* at the junction between occipital cortex and the ventral and dorsal pathways and only these features are represented in higher-order areas for categorization behavior.

Experiment

Our experiment comprised four 2-Alternative-Forced-Choice categorizations of the same original 64 images (8 identities²⁰ representing 2 genders x 2 expressions x 2 vehicles x 2 pedestrian) that each participant (N = 10, within-participant statistics) performed in different blocks of trials. Each trial started with a fixation cross presented for a random time interval [500-1000 ms], followed by one of the original stimuli for 500 ms, whose features were randomly sampled with the Bubbles procedure^{19,21} (see Figure 1A and *Methods, Stimuli*). Bubbles sampling ensures that the participant can only correctly categorize the stimulus when the random samples reveal the features that the participant requires in the task. For example, the random samples of trial *n* in Figure 1A would enable categorization of “happy” in the facial expression block, but not categorization of “SUV” in the vehicle block, and vice versa with the samples of trial *m* (see *Methods, Task Procedure*). Figure 1A illustrates, with two examples, the full set of original images, including all combinations of the task differences (i.e. *face expression, face gender, pedestrian gender and vehicle type*), embedded into the same street scene. Critically, to eliminate all low-level effects due to different stimuli, the set of randomly sampled stimuli was identical in each participant and blocked categorization task (but presented in a random order in each block). We concurrently recorded the participant’s categorization responses and dynamic MEG activity (localized with a beamformer to 5,107 cortical sources, see *Methods, MEG*).

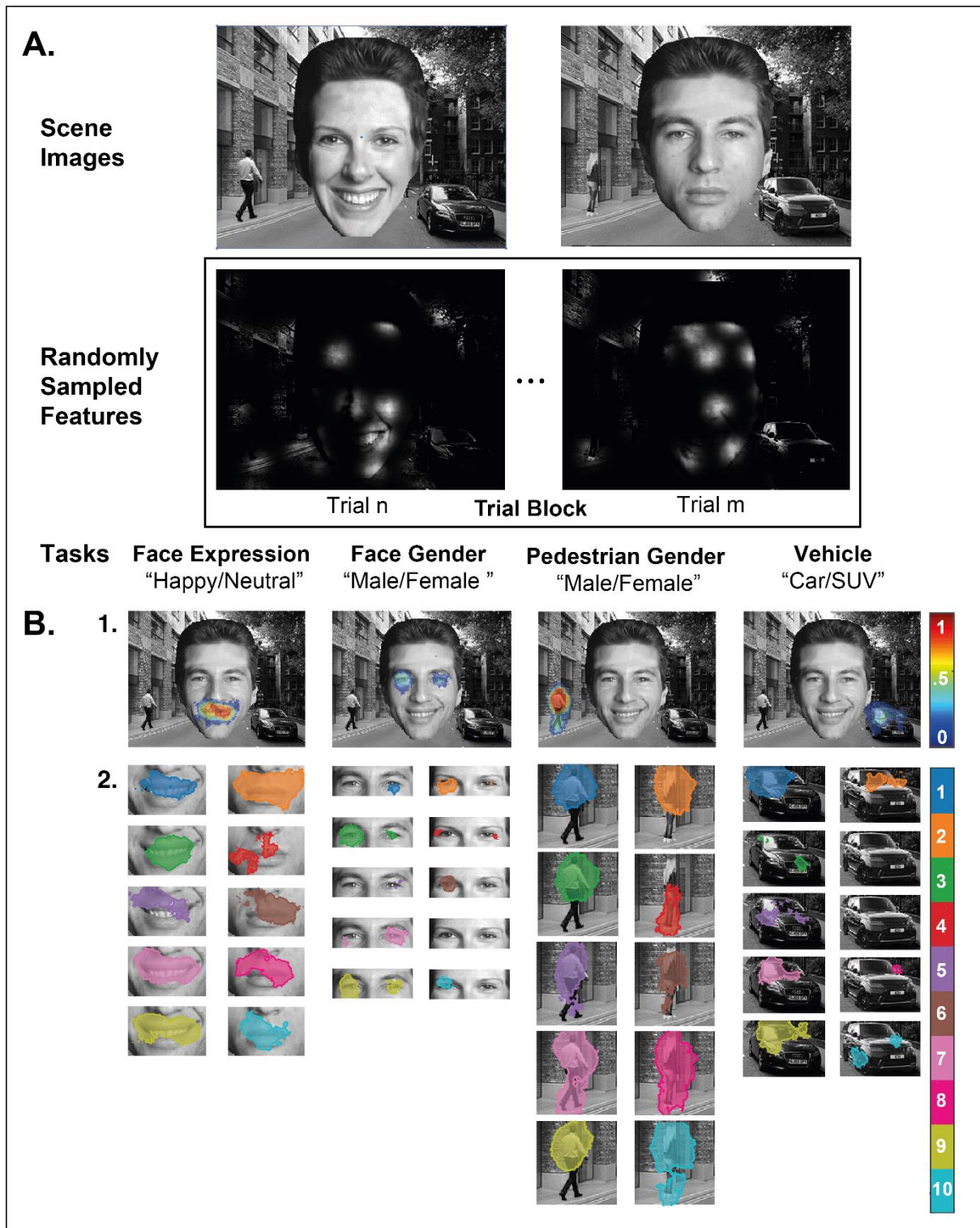


Figure 1. Categorization design and task-relevant features. *A. Experimental design.* We used 64 original images of a street scene that comprises a central face, to its left, a pedestrian on a sidewalk, to its right a parked vehicle. We designed the stimulus set to afford two different categorization responses in each one of four different categorization tasks: *expression* of the central face, with “happy vs. neutral” responses; *face gender* of the central face, “male vs. female”; *pedestrian gender*, “male vs. female”; *vehicle type*, “car vs. SUV.” On each trial, the Bubbles procedure randomly sampled the features of one of the 64 original images to synthesize a bubbled stimulus. We used the same set of bubbled stimuli¹⁹ (presented in a random order) in each task, so that each participant ($N = 10$) saw each bubbled stimulus 8 times (twice per task). *B. Task-relevant*

features by participant. 1. *Bayesian Prevalence.* In each task (columns) and participant, for each image pixel we computed $MI(\langle \text{pixel visibility}; \text{correct vs. incorrect categorization} \rangle)^{22}$, to reveal the significant ($p < 0.05$, FWER corrected) pixels that modulate categorization accuracy. From the proportion of participants who significantly used each pixel, we estimated the population prevalence²³, expressed as a Bayesian maximum a posteriori (MAP) estimate (see legend). 2. *Participant's features.* We expand the results by showing the significant features that each color-coded participant used in each task. Note in each column (e.g. *pedestrian gender*) that different participants can use different (even mutually exclusive) features for the same categorization responses (e.g. for “male” vs “female pedestrian”, upper body in participants 1, 2 and 3; lower body in participant 4).

Results

Behavior: Task-relevant features

Supplementary Tables 1 and 2 report participant-specific categorization performance in each task, which participants resolved well-above chance. To reconstruct the task-relevant features supporting performance, we quantified with Mutual Information ($MI^{22,24}$) the cross-trial relationship between pixel presence vs. absence due to random sampling (Figure 1A) and the participant's corresponding categorization responses in each task—computed as $MI(\langle \text{pixel visibility}; \text{correct vs. incorrect categorization} \rangle)$, controlling the Family Wise Error Rate (FWER) over pixels at $p < 0.05$, see *Methods, Analyses, Participant features*.

Figure 1B.1 illustrates that participants use different features in each categorization task—e.g. to categorize the *expression* of the central face, its mouth features; its *gender*, the left and/or right eye features; *pedestrian gender*, body parts; *vehicle*, different features.

Furthermore, different participants use different features for the same classification of an object—e.g. in Figure 1B.2, participant 1, 7 and 9, use the windshield and a large portion of the front fender and bonnet to determine *vehicle type*, while participant 8 uses the right wing mirror. Importantly, as the sampled stimuli were identical across participants and tasks, Figure 1B.2 isolates the effect of the participant and task on feature selection for behavior. These idiosyncratic stimulus features must be processed by each participant's brain networks to enact the categorization behavior. Having identified these features we can now study where, when and how they do so.

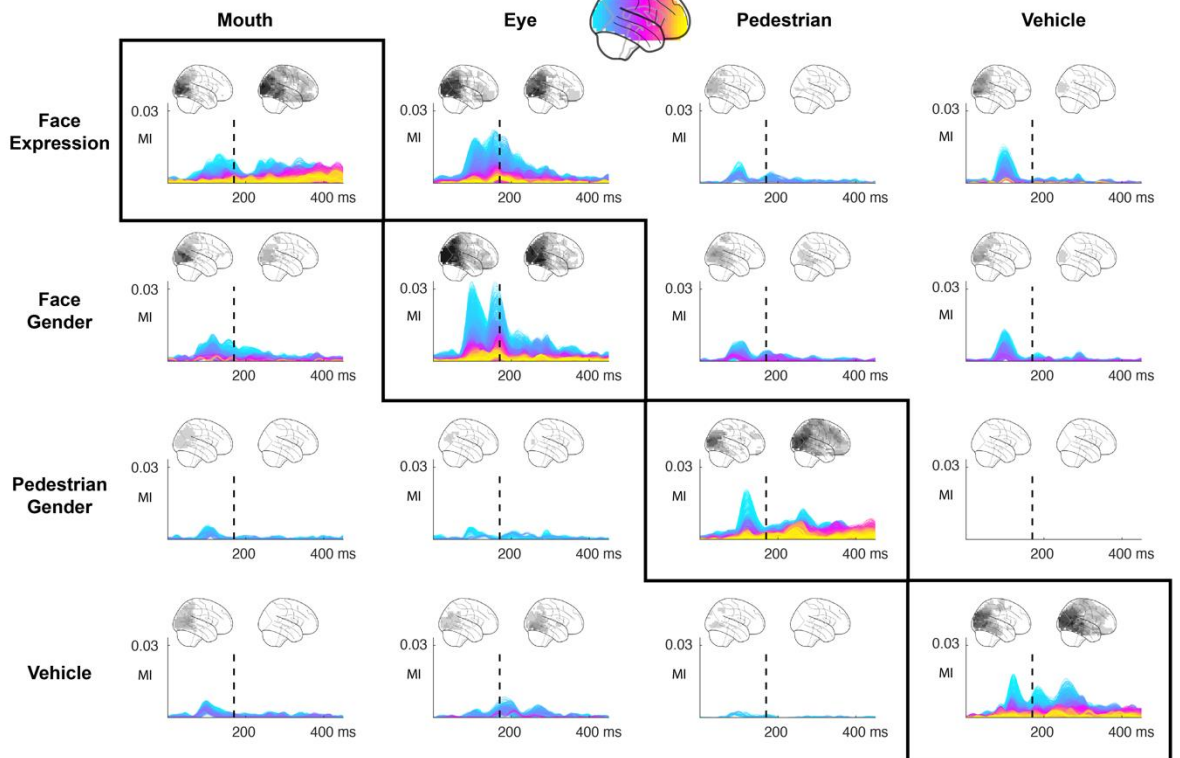
Brain networks: Categorization task modulates representation of the same feature

Note that, by design, each participant feature in Figure 1B.2 is task-relevant for one task (e.g. the blue body part on Figure 1B.2 to categorize *pedestrian gender*) and task-irrelevant for the others (e.g. in *face expression*, *face gender* and *vehicle type*). Therefore, we can directly study where, when and how the task-relevance of a feature modulates its representation (and therefore processing) in the participant's brain activity (i.e. dynamic source-localised MEG responses). To do so, we first derive a per-trial feature visibility score (that we denote F), by intersecting the mask of significant pixels (e.g. the blue mouth in

Figure 2C) with the spatial bubble mask of each randomly sampled stimulus (cf. Figure 1A), resulting in a single value representing the visibility of feature on each trial (see *Methods, Analyses, Feature visibility*). We then computed the statistical dependence between this trial-by-trial variability in feature visibility and the MEG response at each source and time point—i.e. computed as $MI(\langle F; MEG_t \rangle)$ ²², FWER $p < 0.01$, separately within each participant see *Methods, Feature representation on MEG sources*. This quantifies the representation of the feature F at each source and time point. We compute this representation strength during the task where the feature is task-relevant and separately during the tasks where the same feature is not relevant.

The matrix of plots in Figure 2A shows the representational dynamics by feature (columns) and task (rows)—i.e. as the cross-participant average ($N = 10$) of significant MI per MEG source, each color-coded by location on a cyan-to-yellow, occipital-frontal axis, see reference glass brain, every 2 ms post-stimulus. On the diagonal, we can see that task-relevant features (highlighted with boxes, e.g. vehicle feature in *Vehicle*) are represented from occipital to higher-level regions over the full time-course (cf. cyan-to-yellow, occipital-to-frontal time-courses). However, when the same features are irrelevant in the other tasks (cf. the vehicle feature, off the diagonal, the first three rows of the fourth column), they are primarily represented in occipital cortex (cf. cyan curves), prior to 170 ms (cf. dashed reference line of the N170 Event Related Potential associated with multiple visual categorizations^{25–28}). Small brains in Figure 2 locate the population prevalence²³ of these divergent representational effects, showing on each voxel the number of participants who significantly represented each feature, in each task, before vs. after 170ms (cf. left vs. right brains, FWER $p < 0.01$, permutation test, maximum statistic, see *Methods, Feature representation on MEG sources*). A notable exception is the eye features of the central face, that are represented throughout the time course in the two face tasks, whether they are task-relevant or not. We come back to this exception in the General Discussion.

A. MI(F; MEG_t)



B. Synergy(F; MEG_t; Categorizations)

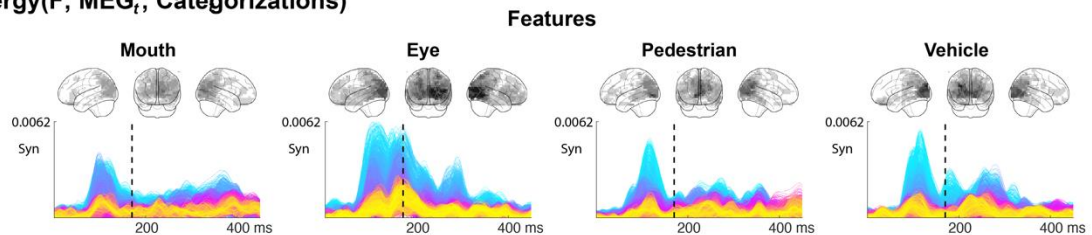


Figure 2. Dynamic representations of the same stimulus feature in different categorization tasks. *A. Dynamic representation of stimulus features (columns) in categorization tasks (rows).* Curves in each cell show the average ($n = 10$ participants) time-course of significant feature visibility representation—of each participant’s feature shown in Figure 2, computed as $MI(\langle F; MEG_t \text{ source amplitude} \rangle)$ ²²—on MEG sources with at least one significant participant, each color-coded by its location on a posterior-to-anterior axis (cyan-yellow) —FWER $p < 0.01$, permutation maximum statistics per participant. Small brains flanking the reference 170 ms dashed line^{25–28} show the feature representation prevalence 50-170 ms post-stimulus (left brain) and 170-450 ms post-stimulus (right brain), Bayesian maximum a posteriori (MAP) population prevalence²³, $n = 10$ participants, $p = 0.01$. Each column reveals qualitatively different representation dynamics of the same stimulus feature when it is task-relevant (matrix diagonal, highlighted with a box) vs. when it is task-irrelevant (off diagonal). *B. Task-modulations of feature representations.* Information theoretic synergy^{22,24} quantifies the overall task-modulation of feature representation. There is strong task-modulation throughout the time course and spatial regions where features are represented. The strongest task-modulation is early in occipital cortex, also at the times of the earliest feature representations.

The columns of Figure 2A shows divergent dynamic representations of the same features on the same MEG sources. We can directly quantify task-modulation by comparing the overall representation of a feature over all tasks, with its representation in specific tasks—ie. computed as information theoretic synergy($\langle F; MEG_t; \text{task} \rangle$), FWER $p < 0.01$ within-

participant maximum statistics, see *Methods, Task modulation of feature representation on MEG sources*. Figure 2B presents this task-modulation measure^{22,24}, showing as above the average of significant time courses across participants, color-coded as in Figure 2A. This shows that task-modulations are ubiquitous, affecting feature representations as early as their ~50 ms onset in occipital cortex (cyan curves, across the matrix of Figure 2A), to their post 170 ms time courses in higher-order regions (pink and yellow curves), but only when features are task-relevant. We investigate these early and late task-modulations on feature representations in more detail next.

In sum, Figure 2A suggests feature representation mechanisms that adaptively select task-relevant features from occipital cortex for higher-level processing. Higher-order areas post 170ms represent primarily task-relevant and not task-irrelevant features (cf. Figure 2A, diagonal highlights vs off-diagonal). The results in Figure 2B confirm that this visible task-modulation via selective representation is statistically significant within individual participants, and further that such task-modulations are pervasive, with strongest peak early in occipital cortex.

Mechanisms of feature selection and reduction

In this section, we develop two key stages of feature processing. To preview, we first investigate the earliest, ~50-170 ms task-modulation in occipital cortex (Figure 2B). We will show that it reflects opponent representations of the same feature when it is task-relevant (and selected, Figure 2A diagonal) vs. irrelevant (and reduced, off-diagonal). Second, we will show that only selected, task-relevant features are later represented in ventral and dorsal regions. This transition ~170 ms reflects a reduction of the dimensionality of stimulus representation from high (in occipital cortex) to low (in the occipito-ventral/dorsal pathways).

Stage 1 (high-dimensional). Opponent representations of task-relevant vs. irrelevant features in occipital cortex

Figure 3B plots the task-modulation time-course of one example occipital source (cyan curve, located in the glass brain), with a 111 ms peak (star on the cyan curve). As shown in Figure 3C, this source represents the same vehicle feature visibility F (cf. Figure 3A) with opposite amplitude responses (Y axis). In the *Vehicle type* task condition (X axis), the source responds with decreasing amplitudes to increasing F (cf. black arrow), whereas in all other tasks, the same source responds to the same F with amplitudes in the opposite direction (cf. grey arrows). Adjacent glass brains generalize from the example and show in source x time the number of participants with at least one such opponent feature representation on each source (FWER $p < 0.01$ corrected over MI-significant sources * 271

time points, see *Methods, Analyses, Opponent feature representations*). Glass brains show how this form of opponency underlies the task-modulation of feature representation in occipital cortex (the first and highest task-modulation peak in Figure 2B). Note that in this early stage, task-relevant and irrelevant features are both represented in occipital cortex, even though task-irrelevant features are not required in the task. However, task-relevance vs. irrelevance incur opponent representations of the same feature visibility F —i.e. a qualitative difference. Therefore, at Stage 1, the stimulus representation is strongly task-modulated, but still higher-dimensional than strictly required to perform the task.

Stage 2 (low-dimensional). Task-relevant feature representations in the rFG

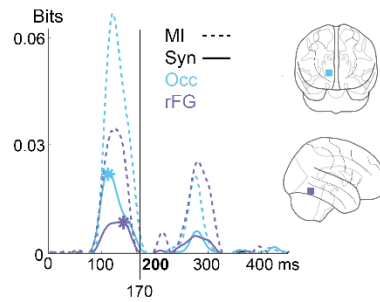
We now characterize in finer spatio-temporal detail the selection of task-relevant features post-170ms shown in Figure 2A. Figure 3B plots the task-modulation curve of one example rFG source (purple curve, located in the glass brain), with a 135 ms peak (star on the curve). As Figure 3D shows, this source now represents feature visibility F in its amplitude responses, but only when the feature is task-relevant. Adjacent glass brains generalize from the example and show in source x time the number of participants with at least one such exclusive task-relevant feature representation (FWER $p < 0.01$ corrected over MI-significant sources * 271 time points, see *Methods, Analyses, Task-relevant feature selection*). Glass brains reveal a later prevalence of these representations in the ventral and dorsal pathways. Note that in Stage 2, post 170 ms, the occipito-ventral/dorsal pathways now primarily process the low-dimensional task-relevant features.

In sum, we have shown a two-stage process. At Stage 1 (~50-170 ms post-stimulus, high-dimensional), occipital cortex processes task-relevant vs task-irrelevant features with opponent representation signatures. At Stage 2 (> 170 ms post-stimulus, low-dimensional), the occipito-ventral/dorsal pathway selects and processes primarily task-relevant features. Enlarged source plots in Figure 3C and 3D reveal the spatio-temporal divergence between Stages 1 (3C) and 2 (3D), ~100-140 ms post-stimulus. We can see that task-irrelevant features are reduced in occipital cortex at the end of Stage 1, whereas task-relevant features are processed thereafter in occipital-ventral (red sources)/dorsal (green sources) pathways. We come back to the implications of these results for theories of attention and recognition in the General Discussion.

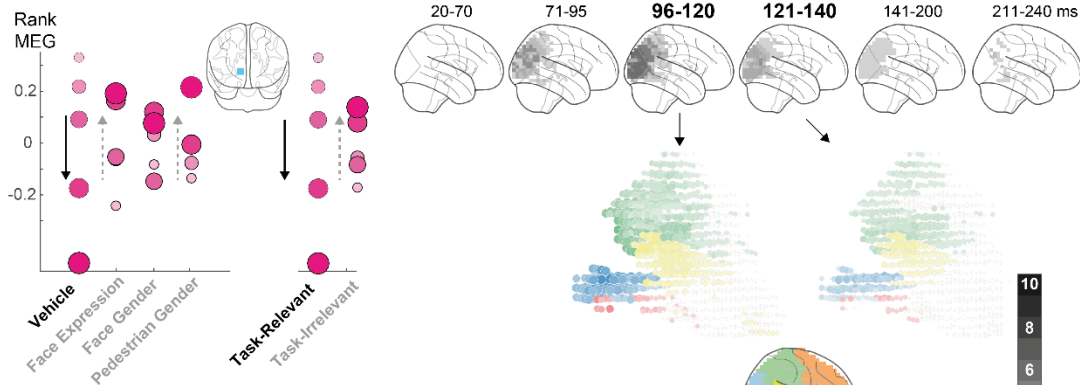
A. F = Feature Visibility



B. Synergy($\langle F; \text{MEG}_t; \text{task-irrelevant} \rangle$)



C. Stage 1: Opponent (Occipital, 111ms*)



D. Stage 2: Task-Relevant (rFG, 135ms*)

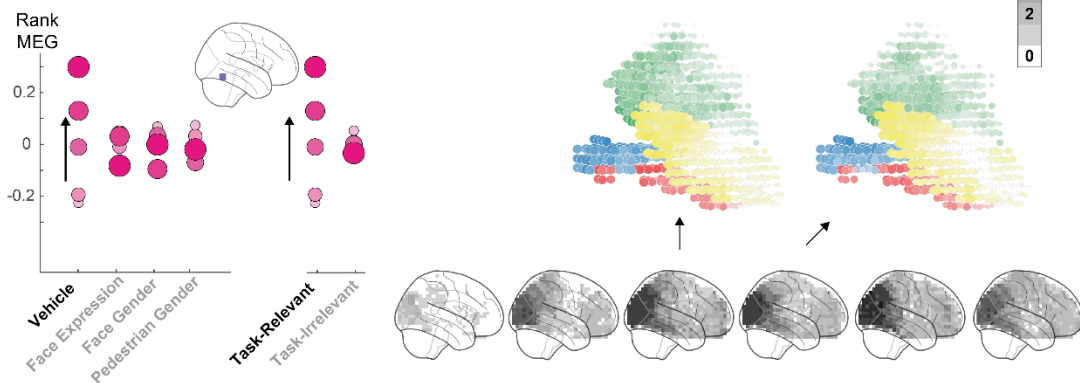


Figure 3. Task-modulations of feature representations. *A. Feature visibility, F.* Random stimulus sampling varies the vehicle feature visibility across trials (participant 8, from Figure 1B.2). *B. Task-modulation of feature representations.* Quantified with synergy^{22,24} for one example occipital source (cyan) and one rFG source (purple) and developed below at peak time (cf. colored stars). *C. Stage 1. Early, opponent occipital representations of gated and reduced features.* Opponent occipital source responses (at 111 ms peak time) to identical F of the vehicle feature (cf. circles of different radii), indicated with arrows in opposite directions, when the feature is task-relevant (i.e. and gated in *Vehicle*, cf. Figure 2) vs. irrelevant (i.e. and reduced in all other categorizations, cf. Figure 2). Adjacent glass brains show the participant numbers with at least one such opponent feature representation on each source within the time window. *D. Stage 2. Later, task-relevant feature representations in the rFG.* The rFG source represents F at 135 ms peak time, but exclusively in the *Vehicle* task. Adjacent glass brains show the number of participants with at least one such exclusive task-relevant feature representation on each source within the time window. Enlarged sources in Figure 3C and 3D reveal the spatio-temporal transition ~100-140 ms post-stimulus, between Stages 1 (3C) and 2 (3D), with occipital cortex (with opponent representations of all features, task-relevant and not, 3C) and ventral (red sources, see colored brain legend) and dorsal (green sources) pathways (with representations of task-relevant features, 3D). Color saturation (i.e. grey-levels) indicate the

prevalence of participants who significantly represent at least one task-relevant vs. irrelevant feature on this source and time window.

Discussion

At a systems-level, we studied the brain network mechanisms that flexibly reduce input dimensionality, by selecting the specific features that support different categorizations of the same stimuli—i.e. *face expression*, *face gender*, *pedestrian gender* and *vehicle type*. In each participant, we reconstructed these task-relevant features and where, when and how brain networks dynamically represent them for behavior. We found pervasive top-down task influences on these representations, starting from the earliest representations of stimulus features in occipital cortex. Specifically, we found that occipital cortex represents stimulus features with opponent signs between ~50-170 ms post-stimulus. When features are task-relevant, they are selected and further represented in the ventral and dorsal stream post 170ms for categorization behavior. However, when these same stimulus features are task-irrelevant, occipital cortex reduces them within 170 ms. Thus, a critical spatio-temporal junction emerges for feature selection ~170 ms, between occipital cortex and the ventral and dorsal streams. Prior to 170 ms, occipital cortex is high-dimensional. It represents all stimulus features with opponent signatures for selection vs. reduction. Following 170 ms, task-irrelevant features have been reduced and the occipito-ventral and dorsal streams are now low-dimensional. They represent exclusively task-relevant features for behavior. We replicated these results in at least 8/10 individual participants of the sample, conferring the feature selection mechanisms a high Bayesian population replication probability.

In psychology and neuroscience, attentional feature selection is the front-end cognitive function of many higher-level theories of face, object and scene categorization and recognition^{1,29}, working^{30–32} and semantic memory^{33,34} and even conscious perception^{35,36}. Before discussing the implications of our results for these theories, we clarify that to realize feature selection, hierarchical layers of the occipital-ventral pathway can feedforward- and feedback-communicate signals, as suggested by models that disambiguate representations across their interactive hierarchical layers^{10,11,37,38}. We generally subscribe to such hierarchical interactive organization, whereby the task (e.g. categorize *vehicle type*) should elicit specific information predictions from memory (i.e. the participant's *vehicle feature*), that propagate down the hierarchy to occipital cortex to meet the input. For example, in our design, different categorization tasks (e.g. *vehicle type* vs. *pedestrian gender*) likely elicited top-down predictions that ascribed opponent representational signatures to the same physical feature variations (i.e. visibility of the *vehicle feature*) in occipital cortex.

The first 170 ms implement attentional selection

Our data are generally compatible with Broadbent's classic early selection model of attention³⁹, whereby task-relevant features are filtered in, whereas task-irrelevant features are filtered out, all within the same early stage of processing. Here, the time course of this early stage is [50-170 ms] post stimulus, for multiple face and object categorizations in a scene, and its primary locus is occipital cortex (likely interacting with higher-level regions). As discussed, attentional selection incurs qualitatively different (i.e. opponent) representations of the same physical feature according to its task-relevance, selection vs. reduction. The broader attention literature discusses interchangeably mechanisms that "filter in/out," "select" and "attend to" features when referring to a capacity-limited cognitive function⁴⁰ that selectively uses task-relevant stimulus information and not others. Our results suggest constraints on the implementation of these mechanisms in brain networks that studies at finer granularities of neural response could further clarify.

Figure 2 illustrates this first constraint, showing that task-relevant features are dynamically represented and maintained throughout the full processing time-course. This raises the question of the gain functions and/or recurrent/interactive activations in the cortical layers (of V1-V4 and the ventral and dorsal pathways) that could actively maintain the representations of various task-relevant features from stimulus onset to behavior. Figure 2 also illustrates the second constraint. Namely, that when these same features become task-irrelevant, occipital cortex still represents them, but only for a short 170 ms duration, and with an opposite sign. Studies that fuse individual MEG source amplitude data with fMRI cortical layer bold responses could similarly address these two constraints by revealing how the inner and outer layers of the occipito-ventral⁴¹⁻⁴³ and dorsal cortex represent the same stimulus features depending on task relevance. This would show how differences in layered cortical activity underlie opponent representations of the same feature for selection or reduction and thereby refine a mechanistic understanding of attentional selection within the first 170ms of stimulus processing.

The 170 ms occipito-ventral/dorsal junction and subsequent visual categorizations

We documented information processes at the occipito-ventral and dorsal junction that distribute before and after the timing and sources of the right occipito-ventral N/M170 Event Related Potentials^{25-28,44-46} (ERPs). Past work already showed that the N/M170 ERP reflects a network that communicates features contra-laterally represented in occipital cortices to the right fusiform gyrus²⁷. A comprehensive reinterpretation of the N/M170 is therefore timely. We showed that the N/M170 peak reflects the junction at which brain networks transition from a first stage of high-dimensional stimulus representation

(comprising all stimulus features) to second lower dimensional stage that only processes task-relevant features. It is therefore not surprising that the N170 has been associated with multiple face, object and scene categorizations^{25–28}. Developing further, the first 170 ms stage could selectively communicate lateralized task-relevant features from the two occipital cortices to the rFG acting as a feature-buffer^{17,27}. The second stage post-170 ms would then integrate^{17,47} these buffered lateralized features into bi-lateral representations for face, body, object and scene categorization behavior. Results of decreasing lateralization of receptive fields⁴⁸ along the occipito-ventral pathway support such bilateral developments of representations.

Here again, further studies could fuse the temporal precision of MEG with the spatial resolution of fMRI^{12,42,43,49} to better understand the cortical layers of the ventral and dorsal pathways that implement the computations that integrate lateralized, buffered features into bilateral “stitched up,” representations of the stimuli, pre- and post-170 ms^{47,50}. When these networks effectively categorize the stimulus is a fundamental question that relates to what visual information is consciously perceived. Our suggestion is that the contents of conscious perception are the categorization features^{51,52}. We come back to this point later.

At this juncture, remember that we flagged one exception to the result that the occipito-ventral and dorsal pathways only process task-relevant features post 170ms. We refer the reader back to Figure 1B.1 and 1B.2, where each participant uses the mouth feature to categorize *face expression*, though the first row of Figure 2A shows that these same participants’ brain networks also represent the eyes of the same face (off the diagonal) throughout the time course, though we know they are not necessary to categorize *face expression*. We documented a similar result over the time-course of the N170 ERP^{44,53}, where the eyes were systematically represented, though not always necessary to judge the expression of a face. Others suggested that the first contact with a face is via the eyes⁵⁴. Our results do indeed suggest that participants represent the eyes and other features of the face in multiple face categorizations. Systematic representations of features spatially distributed across the face into the rFG could explain its apparent “holistic representation”⁵⁵.

Visual categorization of selected stimulus features, memory and conscious perception

As pointed out earlier, attentional selection is often assumed to be the front-end of brain network mechanisms that dispatch specific contents required by other brain mechanisms^{35,36}. For example, our results could illustrate that the occipital cortex communicates task-relevant features to rFG mechanisms that use them to categorize the stimulus^{27,56}. Categorization supposedly compares such featural representations of the input

with featural representations of hierarchically organized categories in memory⁵⁷. Importantly, we have shown that brain networks maintain dynamic representations of task-relevant features from ~50ms until categorization behavior is produced. One fundamental research question is whether and when such maintained representations of task-relevant features (acting as a functional workspace³⁶) are consciously accessed as the contents of perception, in contrast to the reduced task-irrelevant features for which there would be no such conscious access. A fascinating corollary is the specific role of the exclusive representations of task-relevant features post 170 ms in occipital cortex, when they have reached the ventral and dorsal stream. If the format of their communication was a wave of transient task-relevant features travelling through the occipito-ventral and dorsal networks, features would be transiently represented and hierarchically transformed between occipital cortex and behavior (as happens across the layers of a feedforward Deep Neural Network model of categorization⁶). Here, however, the dynamics of our data is more akin to an expanding wave that sustains representations in earlier layers, while reducing task-irrelevant features. Such an expanding representational format could in principle maintain task-relevant information for conscious access to be perceived at high content resolution, from early vision to memory. Future studies should tease apart the specific dynamic format between a travelling wave of transient representations vs. an expanding wave of sustained representations because each format offers a different conception of dynamic perception and conscious access to information contents across hierarchical layers of the visual pathway.

Conclusions

We studied the pervasive mechanisms of dynamic feature selection for flexible visual categorizations. We found that occipital cortex selects or reduces the same feature, depending on its task-relevance, revealing opponent representational signatures at MEG source level within 170ms post-stimulus. Thereafter, occipito-ventral and dorsal networks process exclusively task-relevant features. We discussed the implications of dynamically maintained task-relevant (and reduced task-irrelevant) feature representations across the occipito-ventral and dorsal pathways for theories of attentional selection, face and object categorizations and conscious access to the contents of perception. There emerges a new telescopic model of task-relevant feature processing for categorization and perception that transforms our more typical conception of the travelling wave (e.g. of feedforward Deep Neural Network models of categorization).

References

1. Nosofsky, R. M. Attention, similarity, and the identification–categorization relationship. *Journal of Experimental Psychology: General* **115**, 39–57 (1986).
2. Schyns, P. G. Diagnostic recognition: task constraints, object information, and their interactions. *Cognition* **67**, 147–179 (1998).
3. Gauthier, I., Tarr, M. J., Anderson, A. W., Skudlarski, P. & Gore, J. C. Activation of the middle fusiform ‘face area’ increases with expertise in recognizing novel objects. *Nat Neurosci* **2**, 568–573 (1999).
4. Sigala, N. & Logothetis, N. K. Visual categorization shapes feature selectivity in the primate temporal cortex. *Nature* **415**, 318–320 (2002).
5. Jack, R. E. & Schyns, P. G. Toward a Social Psychophysics of Face Communication. *Annual Review of Psychology* **68**, 269–297 (2017).
6. Daube, C. *et al.* Grounding deep neural network predictions of human categorization behavior in understandable functional features: The case of face identity. *Patterns* **2**, 100348 (2021).
7. Ullman, S. Object recognition and segmentation by a fragment-based hierarchy. *Trends in Cognitive Sciences* **11**, 58–64 (2007).
8. Lindsay, G. W. Convolutional Neural Networks as a Model of the Visual System: Past, Present, and Future. *Journal of Cognitive Neuroscience* **33**, 2017–2031 (2021).
9. de Melo, C. M. *et al.* Next-generation deep learning based on simulators and synthetic data. *Trends in Cognitive Sciences* **26**, 174–187 (2022).
10. Friston, K. The free-energy principle: a unified brain theory? *Nature Reviews Neuroscience* **11**, 127–138 (2010).
11. Yuille, A. & Kersten, D. Vision as Bayesian inference: analysis by synthesis? *Trends in Cognitive Sciences* **10**, 301–308 (2006).
12. Lawrence, S. J. D., Formisano, E., Muckli, L. & de Lange, F. P. Laminar fMRI: Applications for cognitive neuroscience. *NeuroImage* **197**, 785–791 (2019).

13. Henderson, J. M. & Hayes, T. R. Meaning-based guidance of attention in scenes as revealed by meaning maps. *Nat Hum Behav* **1**, 743–747 (2017).
14. Malcolm, G. L., Nuthmann, A. & Schyns, P. G. Beyond Gist: Strategic and Incremental Information Accumulation for Scene Categorization. *Psychol Sci* **25**, 1087–1097 (2014).
15. Brignani, D., Lepsien, J. & Nobre, A. C. Purely endogenous capture of attention by task-defining features proceeds independently from spatial attention. *NeuroImage* **51**, 859–866 (2010).
16. Carrasco, M. & Barbot, A. Spatial attention alters visual appearance. *Current Opinion in Psychology* **29**, 56–64 (2019).
17. Zhan, J., Ince, R. A. A., van Rijsbergen, N. & Schyns, P. G. Dynamic Construction of Reduced Representations in the Brain for Perceptual Decision Behavior. *Current Biology* **29**, 319-326.e4 (2019).
18. Smith, M. L., Gosselin, F. & Schyns, P. G. Measuring Internal Representations from Behavioral and Brain Data. *Current Biology* **22**, 191–196 (2012).
19. Gosselin, F. & Schyns, P. G. Bubbles: a technique to reveal the use of information in recognition tasks. *Vision Research* **41**, 2261–2271 (2001).
20. Dailey, M., Cottrell, G. W. & Reilly, J. California facial expressions, CAFE. *Unpublished digital images, University of California, San Diego, Computer Science and Engineering Department* (2001).
21. Schyns, P. G., Bonnar, L. & Gosselin, F. Show me the features! Understanding recognition from the use of visual information. *Psychological science* **13**, 402–409 (2002).
22. Ince, R. A. A. *et al.* A statistical framework for neuroimaging data analysis based on mutual information estimated via a Gaussian copula. *Human Brain Mapping* **38**, 1541–1573 (2017).
23. Ince, R. A., Paton, A. T., Kay, J. W. & Schyns, P. G. Bayesian inference of population prevalence. *eLife* **10**, e62461 (2021).

24. Cover, T. M. & Thomas, J. A. *Elements of Information Theory*. (John Wiley & Sons, 2012).
25. Bentin, S., Allison, T., Puce, A., Perez, E. & McCarthy, G. Electrophysiological Studies of Face Perception in Humans. *Journal of Cognitive Neuroscience* **8**, 551–565 (1996).
26. Bentin, S. *et al.* Controlling interstimulus perceptual variance does not abolish N170 face sensitivity. *Nature Neuroscience* **10**, 801–802 (2007).
27. Ince, R. A. A. *et al.* The Deceptively Simple N170 Reflects Network Information Processing Mechanisms Involving Visual Feature Coding and Transfer Across Hemispheres. *Cereb Cortex* **26**, 4123–4135 (2016).
28. Rousselet, G. A., Macé, M. J.-M. & Fabre-Thorpe, M. Animal and human faces in natural scenes: How specific to human faces is the N170 ERP component? *Journal of Vision* **4**, 2–2 (2004).
29. Humphreys, G. W. Feature confirmation in object perception: Feature integration theory 26 years on from the Treisman Bartlett lecture. *The Quarterly Journal of Experimental Psychology* **69**, 1910–1940 (2016).
30. van Moorselaar, D. *et al.* Spatially Selective Alpha Oscillations Reveal Moment-by-Moment Trade-offs between Working Memory and Attention. *Journal of Cognitive Neuroscience* **30**, 256–266 (2018).
31. Rhodes, S. & Cowan, N. Attention in working memory: attention is needed but it yearns to be free. *Annals of the New York Academy of Sciences* **1424**, 52–63 (2018).
32. Baddeley, A. The episodic buffer: a new component of working memory? *Trends in Cognitive Sciences* **4**, 417–423 (2000).
33. Grossman, M. *et al.* The Neural Basis for Categorization in Semantic Memory. *NeuroImage* **17**, 1549–1561 (2002).
34. Rubin, D. C. A conceptual space for episodic and semantic memory. *Mem Cogn* **50**, 464–477 (2022).
35. Dehaene, S., Charles, L., King, J.-R. & Marti, S. Toward a computational theory of conscious processing. *Current Opinion in Neurobiology* **25**, 76–84 (2014).

36. Mashour, G. A., Roelfsema, P., Changeux, J.-P. & Dehaene, S. Conscious Processing and the Global Neuronal Workspace Hypothesis. *Neuron* **105**, 776–798 (2020).
37. McClelland, J. L. & Rumelhart, D. E. An interactive activation model of context effects in letter perception: I. An account of basic findings. *Psychological Review* **88**, 375–407 (1981).
38. Kietzmann, T. C. *et al.* Recurrence is required to capture the representational dynamics of the human visual system. *Proceedings of the National Academy of Sciences* **116**, 21854–21863 (2019).
39. Broadbent, D. E. A mechanical model for human attention and immediate memory. *Psychological Review* **64**, 205–215 (1957).
40. Shiffrin, R. M. & Gardner, G. T. Visual processing capacity and attentional control. *Journal of Experimental Psychology* **93**, 72–82 (1972).
41. Margalit, E. *et al.* Ultra-high-resolution fMRI of Human Ventral Temporal Cortex Reveals Differential Representation of Categories and Domains. *J. Neurosci.* **40**, 3008–3024 (2020).
42. Huber, L. *et al.* Layer-dependent functional connectivity methods. *Progress in Neurobiology* **207**, 101835 (2021).
43. Self, M. W., van Kerkoerle, T., Goebel, R. & Roelfsema, P. R. Benchmarking laminar fMRI: Neuronal spiking and synaptic activity during top-down and bottom-up processing in the different layers of cortex. *NeuroImage* **197**, 806–817 (2019).
44. Schyns, P. G., Petro, L. S. & Smith, M. L. Dynamics of visual information integration in the brain for categorizing facial expressions. *Current biology* **17**, 1580–1585 (2007).
45. Rousselet, G. A., Ince, R. A. A., Rijsbergen, N. J. van & Schyns, P. G. Eye coding mechanisms in early human face event-related potentials. *Journal of Vision* **14**, 7–7 (2014).
46. Healthy aging delays the neural processing of face features relevant for behavior by 40 ms - Jaworska - 2020 - Human Brain Mapping - Wiley Online Library.
<https://onlinelibrary.wiley.com/doi/full/10.1002/hbm.24869>.

47. Jaworska, K., Yan, Y., van Rijsbergen, N. J., Ince, R. A. & Schyns, P. G. Different computations over the same inputs produce selective behavior in algorithmic brain networks. *eLife* **11**, e73651 (2022).
48. Kay, K. N., Weiner, K. S. & Grill-Spector, K. Attention Reduces Spatial Uncertainty in Human Ventral Temporal Cortex. *Current Biology* **25**, 595–600 (2015).
49. Finn, E. S., Huber, L. & Bandettini, P. A. Higher and deeper: Bringing layer fMRI to association cortex. *Progress in Neurobiology* 101930 (2020)
doi:10.1016/j.pneurobio.2020.101930.
50. Schyns, P. G., Gosselin, F. & Smith, M. L. Information processing algorithms in the brain. *Trends in Cognitive Sciences* **13**, 20–26 (2009).
51. Schyns, P. G. & Oliva, A. From blobs to boundary edges: Evidence for time- and spatial-scale-dependent scene recognition. *Psychological science* **5**, 195–200 (1994).
52. Schyns, P. G. & Oliva, A. Dr. Angry and Mr. Smile: When categorization flexibly modifies the perception of faces in rapid visual presentations. *Cognition* **69**, 243–265 (1999).
53. Schyns, P. G., Jentzsch, I., Johnson, M., Schweinberger, S. R. & Gosselin, F. A principled method for determining the functionality of brain responses. *NeuroReport* **14**, 1665–1669 (2003).
54. Niedenthal, P. M., Mermillod, M., Maringer, M. & Hess, U. The Simulation of Smiles (SIMS) model: Embodied simulation and the meaning of facial expression. (2010)
doi:10.18452/23061.
55. Richler, J. J. & Gauthier, I. A meta-analysis and review of holistic face processing. *Psychological Bulletin* **140**, 1281–1302 (2014).
56. Ince, R. A. A. *et al.* Tracing the Flow of Perceptual Features in an Algorithmic Brain Network. *Scientific Reports* **5**, 17681 (2015).
57. Murphy, G. L. *The big book of concepts*. (MIT Press, 2002).
58. Oostenveld, R., Fries, P., Maris, E. & Schoffelen, J.-M. FieldTrip: Open Source Software for Advanced Analysis of MEG, EEG, and Invasive Electrophysiological Data. *Computational Intelligence and Neuroscience* **2011**, e156869 (2010).

59. Gross, J. *et al.* Good practice for conducting and reporting MEG research. *NeuroImage* **65**, 349–363 (2013).
60. Hillebrand, A. & Barnes, G. R. Beamformer Analysis of MEG Data. in *International Review of Neurobiology* vol. 68 149–171 (Academic Press, 2005).
61. Lancaster, J. L. *et al.* Automated Talairach atlas labels for functional brain mapping. *Hum Brain Mapp* **10**, 120–131 (2000).

Acknowledgments

PGS was supported by the EPSRC [MURI 1720461] and the Wellcome Trust [107802]. PGS is a Royal Society Wolfson Fellow [RSWF\R3\183002]. RAAI was supported by the Wellcome Trust [214120/Z/18/Z].

Methods

Participants

Ten participants with normal or corrected to normal vision participated in all four tasks and gave informed consent. The experiment was conducted in University of Münster, Germany. The study was approved by the ethics committee of the University of Münster (2019-198-f-S) and conducted in accordance with the Declaration of Helsinki.

Stimuli

We used 64 original greyscale images (8 face identities × 2 expressions × 2 pedestrians × 2 car) of a realistic city street scene comprising the combinations of varying embedded targets: a central face (which was male vs. female and happy vs. neutral), left flanked by a pedestrian (male vs. female), right flanked by a parked vehicle (car vs. SUV). The images were presented at 5.72° × 4.4° of visual angle, with 364 × 280 pixel size. We sampled information from each image, using the Bubbles procedure. Specifically, we multiplied the image with randomly positioned Gaussian apertures (sigma = 15 pixels) to vary the visibility of image features on each trial. We pre-generated 768 random bubble masks which were the same in all categorization tasks. On each session of trials, we applied the 768 masks to 12 repetitions of the original 64 images, for a total of 768 trials presented in a random order.

Task procedure

Each trial began with a fixation cross displayed for 5 ms, immediately followed by one of bubble masked stimuli displayed for 500 ms. Participants were instructed to maintain fixation on each trial and respond as quickly and accurately as possible, by pressing one of two keys ascribed to each response choice—i.e. “happy” vs. “neutral” in *face expression*; “male” vs. “female” in *face gender* task; “male” vs. “female” in *pedestrian gender*; “car” vs. “SUV” in *vehicle type*. Each task comprised two sessions of trials, each comprising 768 trials (of 6 runs followed by a short break, each run comprising 128 trials = 8 identities × 2 expressions × 2 pedestrians × 2 cars × 2 repetitions).

MEG

Participants were seated upright in a magnetically shielded room while we simultaneously recorded MEG and behavior data. Brain activity was recorded using a 275 channel whole-head MEG system (OMEGA 275, VSM Medtech Ltd., Vancouver, Canada) at a sampling rate of 600 Hz. During MEG recordings, head position was continuously tracked online by the CTF acquisition system. For MEG source localization, we obtained high-resolution structural magnetic resonance imaging (MRI) scans in a 3T Magnetom Prisma scanner (Siemens, Erlangen, Germany).

Pre-processing

We performed analyses with Fieldtrip⁵⁸ and in-house MATLAB code, following recommended guidelines⁵⁹. We first visually identified noisy channels and trials with epoched data (-400 to 1500 ms around stimulus onset on each trial) high-pass filtered at 1 Hz (4th order two-pass Butterworth IIR filter). Next, we epoched the raw data into trial windows (-400 to 1500 ms around stimulus onset, 1-25 Hz band-pass, 4th order two-pass Butterworth IIR filter), filtered for line noise (notch filter in frequency space), applied fieldtrip build-in denoise function specific to the MEG system, and rejected noisy channels and trials identified in the first step. We then decomposed the data with ICA, and visually identified and removed the independent component corresponding to artifacts (eye blinks or movements, heartbeat).

Source reconstruction

We applied a Linearly Constrained Minimum Variance (LCMV) beamformer⁶⁰ to reconstruct the time series of 12,773 sources on a 6mm uniform grid warped to standardized MNI coordinate space. Using a Talarach-Daemon atlas⁶¹, we excluded all cerebellar and non-cortical sources, and performed statistical analyses on the remaining 5,107 cortical grid sources. We categorized cortical sources into four regions based on ROIs defined in the Talarach-Daemon atlas⁶¹.

Table 1. Cortical sources categorized into four regions of the Talarach-Daemon atlas⁶¹.

Occipital region	Lingual gyrus (LG) Cuneus (CUN) Inferior Occipital Gyrus (IOG) Middle Occipital Gyrus (MOG) Superior Occipital Gyrus (SOG)
Temporal region	Fusiform Gyrus (FG) Inferior Temporal Gyrus (ITG)

	Middle Temporal Gyrus (MTG) Superior Temporal Gyrus (STG)
Parietal region	Superior Parietal Lobule (SPL) Inferior Parietal Lobule (IPL) Angular Gyrus (ANG) Supramarginal Gyrus (SMRG) Precuneus (PRECUN) Postcentral Gyrus (POSTCEN)
Frontal region	Anterior Cingulate (AC) Inferior Frontal Gyrus (IFG) Medial Frontal Gyrus (MeFG) Middle Frontal Gyrus (MiFG) Orbital Gyrus (OG) Paracentral Lobule (PL) Precentral Gyrus (PRECEN) Superior Frontal Gyrus (SFG)

Analyses

Participant features

To reveal what image features each participant used to in each categorization task (i.e. the task-relevant features), we quantified the statistical dependence between the visibility of each pixel (due to bubbles sampling¹⁹ on each trial) and the corresponding correct vs. incorrect response of the participant in this task, computed as Mutual Information^{22,24}, $MI(\langle \text{pixel visibility}; \text{correct vs. incorrect categorization} \rangle)$. We represented pixel visibility on each trial as a real number from 0 to 1 (low to high visibility), which we then binarized using a 0.2 threshold into 2 categories: 0 for low visibility and 1 for high visibility. To establish statistical significance, we ran a non-parametric permutation test with 1,000 shuffled repetitions, corrected over 364 x 280 pixels using maximum statistics (FWER $p < 0.05$). Significant pixels represent the participant's task-relevant features whose visibility influences their categorization behavior in each task (see Figure 1B).

Feature visibility

As different participants can use different features in each task, to generalize analyses across participants, we transformed the data from levels of pixel visibility into levels of feature visibility (i.e. comprising the pixels making up the features of each participant). To

this end, for each feature we selected the top 5% pixels with highest MI(<pixel visibility; correct vs. incorrect categorization>) to form feature masks. On each trial, we computed feature visibility as the feature mask pixels shown by the bubbles sampling, weighted by the MI values of each pixel of the feature mask. We divided mouth (for *face expression*) and eyes (for *face gender*) features into their left and right components and considered them as a 2-dimensional feature variable in our analyses. Figure 1B shows the feature masks of each participant and task.

Feature representation on MEG sources

To reconstruct where, when and how MEG sources represent each participant's features, we computed MI between the visibility of each feature and 5107 MEG source signals over 0 to 450 ms, in each task—i.e. when the feature is task-relevant, and also in the three other tasks when it is task-irrelevant, computed as MI(<feature visibility; MEG_t>) with a Gaussian Copula²². To establish statistical significance, we ran a non-parametric permutation test with 1,000 shuffled repetitions, corrected (FWER $p < 0.01$) over 5107 sources x 271 timepoints with maximum statistics. This computation produces a 4 (tasks) x 4 (features) x 5,107 sources x 271 time points feature representation matrix for each participant.

Task modulation of feature representation on MEG sources

Synergy computes the difference between the overall representation strength of a feature (i.e. its visibility, F) in MEG activity, quantified across all trials ignoring the particular task (quantified with MI), and the average task-conditional representation strength (quantified with conditional MI):

$$\text{Synergy}(\langle F; \text{MEG}_t; \text{Task} \rangle) = \text{MI}(\langle F; \text{MEG}_t \mid \text{Task} \rangle) - \text{MI}(\langle F; \text{MEG}_t \rangle)$$

If task has no effect on representation these quantities will not differ resulting in zero synergy. Synergy results when the average strength of representation is higher when controlling for task—meaning that an observer trying to predict the stimulus from brain activity will perform better if they also know the task performed.

To quantify the modulation effect of the four categorization tasks on the representation of the participant's features into MEG source activity, for each participant feature, we computed information theoretic synergy, as just defined, between 0 and 450 ms post-stimulus, where the categorization tasks variable has values of 1 to 4 to represent each task. To establish statistical significance, we use a nonparametric permutation test, with 1,000 repetitions, shuffling the task label of each trial, corrected over 5107 sources * 271 timepoints (FWER p

< 0.01). This provides permutation samples from the null distribution where task does not affect feature representation.

Task-relevant vs. task-irrelevant

To quantify the specific modulation of task-relevance vs. irrelevance on the MEG source representation of each participant feature, we computed again synergy, this time as synergy(<feature visibility; MEG_i; task-relevance>), where task-relevance could be 1 (for task-relevant) or 2 (for task-irrelevant). We observed synergy arising from two different representational mechanisms: Opponent feature representation and task-relevant feature selection. We define each below.

Opponent feature representations: Occurs when a given source significantly represents a participant feature with a particular sign of feature-MEG correlation when the feature is task-relevant, and an opposite sign when irrelevant. This means there is significant MI feature representation in multiple tasks, but their synergy reveals that the form of this representation is task-specific.

We formalize this effect as the following logical conjunction (see Figure 3C):

Opponent feature representation:-

<significant task-relevant MI>
& <task-irrelevant MI>
& <significant synergy>
& <opponent signs for relevant vs irrelevant>

Task-relevant feature selection: Occurs when a given source represents a participant feature only when it is task-relevant. This synergy is logically defined as (see Figure 3D):

Task-relevant feature selection:-

<significant task-relevant MI>
& <no significant task-irrelevant MI>
& <significant synergy>

Bayesian population prevalence

Table 2 below provides a reference to transform the proportion of participants from the sample who have a significant effect into the Bayesian population prevalence²³. Population prevalence is a Bayesian estimate of the within-participant replication probability. Replicating

a result in multiple participants offers a much higher standard of evidence than to declare statistical significance of a population mean effect. For example, $p = 0.05$ typically defines population mean statistical significance; $p < 0.001$ would be considered stronger evidence. In Figure 3A (diagonal of the matrix), we show 8/10 participants have significant MI task-relevant feature representations in occipital and ventral cortex (FWER $p < 0.01$). The frequentist p-value corresponding to this result under the global null that no one in the population shows this effect is 1.6×10^{-9} . Under the global null our results are therefore 7 orders of magnitude more surprising than a typical mean demonstrating the experimental effect at the population level. Here, we report Bayesian estimates of the population parameter with their associated uncertainty. Given 8/10 participants significant at $p = 0.01$, we can be confident that the population replication probability is greater than 49%. We would expect the majority of the population to show this result if they were tested in the same experiment.

Table 2. Bayesian population prevalence: Maximum A Posteriori (MAP) [95% Highest Posterior Density Interval (HPDI)] for k significant participants out of 10.

	Within participant $\alpha = 0.05$	Within participant $\alpha = 0.01$
K=10	1 [0.75 - 1]	1 [0.75 - 1]
K=9	0.89 [0.61 - 0.99]	0.90 [0.61 - 0.99]
K=8	0.79 [0.49 - 0.96]	0.80 [0.49 - 0.96]
K=7	0.68 [0.38 - 0.90]	0.70 [0.38 - 0.90]
K=6	0.58 [0.28 - 0.83]	0.60 [0.28 - 0.83]
K=5	0.47 [0.19 - 0.75]	0.49 [0.19 - 0.75]
K=4	0.37 [0.11 - 0.66]	0.39 [0.11 - 0.66]
K=3	0.26 [0.05 - 0.56]	0.29 [0.05 - 0.56]
K=2	0.16 [0 - 0.44]	0.19 [0 - 0.44]
K=1	0.05 [0 - 0.34]	0.09 [0 - 0.34]

Supplementary Tables

Supplementary Table 1 reports the average categorization accuracy and reaction time performance (standard deviation in parentheses) in each task of the design (see Supplementary Table 2 below for individual participants' data).

Supplementary Table 1. Average accuracy and reaction times across participants in each categorization task.

	Expression	Face Gender	Pedestrian Gender	Vehicle
Accuracy	77.21% (1.45%)	75.12% (1.92%)	76.11% (1.56%)	65.25% (1.91%)
Reaction Time	753 ms (54.14)	738 ms (42.24)	779 ms (42.15)	978 ms (50.51)

Supplementary Table 2. Per participant average accuracy and RT in each categorization task.

	Expression	Gender (face)	Gender(pedestrian)	Vehicle
Participant 1	70.31%	68.82%	75.20%	69.01%
Participant 2	78.06%	74.61%	73.57%	64.19%
Participant 3	83.59%	85.74%	80.99%	55.17%
Participant 4	76.63%	74.22%	67.84%	57.23%
Participant 5	76.30%	74.35%	71.74%	60.35%
Participant 6	76.17%	71.81%	74.35%	66.80%
Participant 7	84.44%	83.07%	83.07%	66.54%
Participant 8	70.64%	65.36%	79.62%	67.84%
Participant 9	78.26%	75.46%	73.31%	72.07%
Participant 10	77.67%	77.73%	81.38%	73.31%

	Expression (ms)	Face-Gender	Pedestrian Gender	Vehicle
Participant 1	614	583	651	775
Participant 2	1127	954	1058	1308
Participant 3	654	690	730	846
Participant 4	805	729	796	1037
Participant 5	865	903	824	890
Participant 6	684	816	745	1037

Participant 7	667	642	668	790
Participant 8	614	683	650	821
Participant 9	596	554	725	928
Participant 10	906	828	946	946